PHOTOMETRIC PROPERTIES OF LUNAR TERRAINS DERIVED FROM HAPKE'S EQUATION.
Paul Helfenstein and Joseph Veverka, Center for Radiophysics and Space Research, Cornell University, Ithaca, NY 14853-6801.

Hapke's bidirectional reflectance equations [1,2,3] provide the most rigorous available description of photometric behavior in terms of physically meaningful parameters. In the newest version [3], six model parameters characterize photometric properties: The efficiency with which average particles scatter and absorb light is described by single scattering albedo, w. The opposition effect, a surge in brightness observed in particulate surfaces near zero phase [4,5,6,7, 8,9,10] is characterized by two parameters; h, which relates its angular width to the combined effects of regolith compaction and particle size distribution, and S(0), the contribution of singly scattered light primarily by first-surface reflection at zero phase. The particle phase function is a Legendre polynomial with first and second order coefficients b and c, respectively. Finally, $\bar{\theta}$, is an average topographic slope angle providing a measure of sub-resolution scale macroscopic roughness.

The complexity of Hapke's equation and comparatively large number of model parameters makes the unique solution of meaningful parameter values difficult. Reliable methods for simultaneously solving all six parameters from remotely-sensed data needs development and testing. The primary objective of this study is to derive Hapke parameters for the lunar surface from both disk-integrated and disk-resolved photometric data. The Moon is the only extraterrestrial body for which samples have been returned to Earth for laboratory analysis, for which extensive manned and unmanned geological field observations have been conducted, and for which corresponding regional photometric measurements have been obtained over adequate ranges of illumination and viewing geometry. The derivation of physically and geologically meaningful parameters from the existing lunar photometric data set is an important test of the usefulness of Hapke's equation in remote sensing applications where surface-based ground truth measurements are unavailable. Hapke's parameters for the Moon also provide a foundation for the comparison of parameters derived from other planetary surfaces.

Visual disk-integrated phase curve data were obtained by renormalizing and combining the measurements of Russell [11,12], Rougier [13], and Shorthill et al. [14] to the precise photoelectric measurements of Lane and Irvine [15], which covered a slightly smaller range of phase angles. The combined data were subdivided and averaged in phase angle bins having the following intervals: data in the range of 0°- 10° were divided into 2.5° bins, data in the range of 10° - 30° were divided into 5° bins, and data in the range of 30° to 150° were divided in 10° bins. Lunar disk-resolved reflectance data were a subset of the extensive measurements tabulated by Shorthill et al. [14] who divided terrains into three groups on the basis of their normal albedoes, A_n. We have preserved their classification system and used data for thirty-two dark lunar terrains ($0.06< A_n <0.09$), twenty-five average terrains ($0.10< A_n <0.12$), and thirty bright terrains ($0.13< A_n <0.16$) in their catalogue. We combined all similar terrain classes into three groups and renormalized all brightness measurements to group-mean albedoes. Average brightnesses, incidence angles (i), and emission angles (e) were determined at each phase angle (α) in each group.

Hapke's equation was fit to the disk-integrated phase curves and disk-resolved data for dark, average, and bright terrain classes using an iterative, non-linear least-squares algorithm described by Helfenstein [16]. Parameters were initially determined from the disk-integrated data, and the result was applied as a first-guess to the iterative solution of parameters for individual terrain classes. Table 1 lists our numerical results. The visual phase curve computed from the best-fit is presented with the averaged disk-integrated data in Figure 1. Figure 2 shows plots of the disk-resolved data normalized to corresponding brightnesses predicted from the disk-integrated solution under the same illumination and viewing geometries. The curves in Figure 2 represent the similarly normalized brightnesses predicted from disk-resolved solutions for all points such that $i=e=\alpha/2$.

Disk-integral photometric properties of the Moon and Mercury at visual wavelengths are known to be remarkably similar [17]. Our value of w, S(0), b, and $\bar{\theta}$ are nearly identical to those found by Veverka et al. [18] for Mercury. Our value of h (0.07) falls in between Veverka et al.'s Mercurian value (0.08) and the 0.05 value derived from lunar farside data [19] by Hapke [3]. Disk-integrated and disk-resolved solutions are mutually consistent. The value of each disk-integrated parameter lies between end-member dark and bright terrain values, and does not differ strongly from the average albedo terrain value.

Systematic trends in disk-resolved parameters can be identified in Table 2. Not surprisingly, values for single scattering albedo (w) of the dominantly anorthositic average and bright terrains are significantly larger than the value for the basaltic dark terrains (mare). Decreasing values of b for dark through

LUNAR PHOTOMETRY

Helfenstein, Paul and Veverka, J.

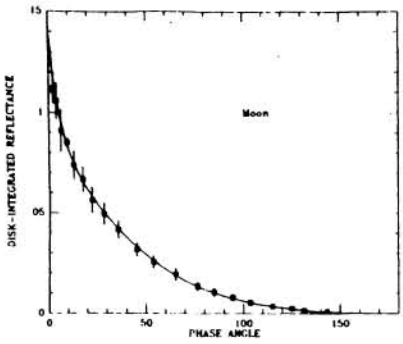

Table 1: Hapke Parameters for Lunar Terrains

	w	h	S(0)	b	c	$\bar{\theta}$
Disk-Integrated	0.21	0.07	0.71	0.29	0.39	20.0°
Disk-Resolved Dark	0.12	0.12	0.51	0.41	0.10	8.1°
Disk-Resolved Average	0.25	0.06	0.78	0.33	0.37	20.6°
Disk-Resolved Bright	0.33	0.05	1.03	0.26	0.45	24.0°

Figure 1 (left): Predicted lightcurve and averaged disk-integrated data (one sigma error bars), normalized to geometric albedo at zero phase.

Figure 2 (bottom): Averaged disk-resolved data normalized to predicted brightness from disk-integrated solution. a) dark terrains, b) average terrains, c) bright terrains. Curves represent predicted normalized brightnesses for hypothetical points on the surface such that $i=e=\alpha/2$.

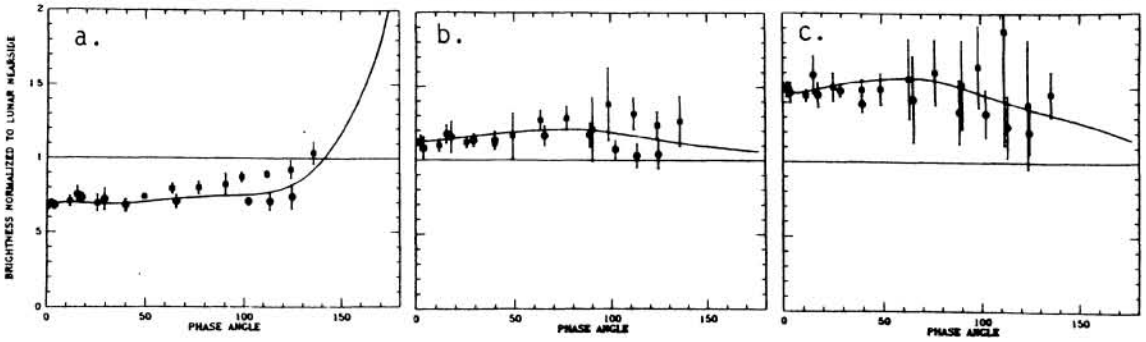

bright terrains indicate that dark regoliths are, as expected, more backscattering than those in average and bright lunar terrains. Values of h likewise decrease from dark through bright terrains indicating that the angular width of the opposition effect is greatest for mare. This would suggest either that mare soils have lower surface porosities, or that they have a slightly different characteristic regolith particle-size distribution. Since porosities over most of the lunar surface are known to be remarkably similar (~45%) [20,21,22], the difference is most likely due to a greater abundance of fine grains (<20 μm) in lunar highlands regoliths [23]. The total amplitude of the opposition surge, $B_0 = S(0)/w\{1+b+c\}$, for dark terrains is larger than for average and bright terrains. This appears to be a consequence of the fact that in opaque particles a larger fraction of singly scattered light at zero phase comes from first surface reflection, S(0). The average macroscopic roughness ($\bar{\theta}$) of dark terrain is significantly lower than that of average and bright terrains. The ratio of of $\bar{\theta}$ for bright terrain to $\bar{\theta}$ for dark terrain is 2.5. This value corresponds to subcentimeter scales and compares well to the ratio of 2.0 derived from radar RMS slopes of highland (β=8°) and mare (β=4°) at 13 cm wavelengths [24].

Acknowledgement: This research was supported by NASA grant NSG-7606.

REFERENCES: [1] Hapke, B. (1981) JGR 86, 3039-3054. [2] Hapke, B.(1984) Icarus 59, 41-59. [3] Hapke, B. (1986) Icarus 67, 264-280. [4] Seeliger, H.(1887) Abhandl. Bayer. Akad. Wiss. Math.-Natur. 16, 405-516. [5] Seeliger, H. (1895) Abhandl. Bayer. Akad. Wiss. Math. Natur. 18, 1-72. [6] Hapke, B. (1963) JGR 68, 4571-4576. [7] Hapke, B. (1966) Astrophys. J. 71., 333-339. [8] Bobrov, M. (1970) In Surfaces and Interiors of Planets and Satellites, Acad. Press, NY. [9] Gehrels, T., et al., (1964) Astron. J. 69, 826-852. [10] Irvine, JGR 71, 2931-2937. [11,12] Russell, H. (1916) Astrophys. J. 43, 103 & 173. [13] Rougier, M. (1933) Ann. Obs. Strasbourg 2, 205-339. [14] Shorthill, R., et al., (1969) NASA Contr. Rep. CR-1429, 405 pp. [15] Lane, A. and W. Irvine (1973) Astrophys. J. 78, 267-277. [16] Helfenstein, P.(1986) Ph.D. Thesis, Brown Univ.,Providence, RI, 414 pp. [17] Hapke, B. (1977) Physics of Earth and Planet. Interiors 15, 264-274. [18] Whitaker, E. (1979) Icarus 40, 406-417. [19] Veverka, J. et al., (1986) in preparation. [20] Houston, W., et al.(1972) Proc. LPSC III, 3255-3263. [21] Carrier, W., et al.(1972) Proc. LPSC III, 3223-3234. [22] Carrier, W., et al.(1974) Proc. LPSC V, 2361-2364. [23] McKay, D., et al.(1974) Proc. LPSC V, 887-906. [24] Tyler, G. (1979) Icarus 37, 29-45.